REPORT DOCUMENTATION PAGE

Form Approved
OMB No. 0704-0188

PLEASE DO NOT RETURN YOUR FORM TO THE ABOVE ORGANIZATION.

1. REPORT DATE *(DD-MM-YYYY)*	2. REPORT TYPE	3. DATES COVERED *(From - To)*
11-05-2015	Confernce Proceedings	

4. TITLE AND SUBTITLE

ARE THE SATELLITE-OBSERVED NARROW, STREAKY CHLOROPHYLL FILAMENTS LOCALLY INTENSIFIED BY THE SUBMESOSCALE PROCESSES?

5a. CONTRACT NUMBER

5b. GRANT NUMBER

5c. PROGRAM ELEMENT NUMBER

0602435N

6. AUTHOR(S)

Igor Shulman, Bradley Penta, James Richman, Gregg Jacobs, Stephanie Anderson, Peter Sakalaukus

5d. PROJECT NUMBER

5e. TASK NUMBER

5f. WORK UNIT NUMBER

73-4877-05-5

7. PERFORMING ORGANIZATION NAME(S) AND ADDRESS(ES)

Naval Research Laboratory
Oceanography Division
Stennis Space Center, MS 39529-5004

8. PERFORMING ORGANIZATION REPORT NUMBER

NRL/PP/7330--15-2499

9. SPONSORING/MONITORING AGENCY NAME(S) AND ADDRESS(ES)

Office of Naval Research
One Liberty Center
875 North Randolph Street, Suite 1425
Arlington, VA 22203-1995

10. SPONSOR/MONITOR'S ACRONYM(S)

ONR

11. SPONSOR/MONITOR'S REPORT NUMBER(S)

12. DISTRIBUTION/AVAILABILITY STATEMENT

Approved for public release, distribution is unlimited.

13. SUPPLEMENTARY NOTES

14. ABSTRACT

Based on observations and modeling studies we have evaluated the impact of submesoscale processes on the development and intensification of offshore narrow (5-10km wide) phytoplankton filaments during summer time in the Monterey Bay, CA. We have demonstrated that, submesoscale processes (surface frontogenesis and nonlinear Ekman transport) lead to the development of very productive phytoplankton patches along the edges between the cold jet and warm anticyclonic eddy. Our results illustrate that during persistent upwelling favorable winds, submesoscale processes can modulate the development and intensification of offshore narrow (5-10km wide) phytoplankton filaments. These processes can incubate the phytoplankton population offshore (as for example, bioluminescent dinoflagellates during August 2003). These offshore phytoplankton filaments can migrate onshore during relaxed winds following the upwelling, and be an additional source of phytoplankton bloom development in and around Monterey Bay. Therefore, the discussed offshore phytoplankton filaments may be a factor in the Bay ecosystem health, as for example, in the development of such events as harmful algae blooms (HABs). All these emphasize the importance of further observational and modeling studies of these submesoscale processes which impact the development and intensification of offshore phytoplankton filaments.

15. SUBJECT TERMS

Coastal Processes, Submesoscale Processes, Phytoplankton Filaments, Interdisciplinary Oceanography

16. SECURITY CLASSIFICATION OF:			17. LIMITATION OF ABSTRACT	18. NUMBER OF PAGES	19a. NAME OF RESPONSIBLE PERSON
a. REPORT	b. ABSTRACT	c. THIS PAGE			Igor Shulman
Unclassified	Unclassified	Unclassified	UU	14	19b. TELEPHONE NUMBER *(Include area code)* (228) 688-5646

Reset

PUBLICATION OR PRESENTATION RELEASE REQUEST

15-123-0743

Publ[illegible] 7[illegible] (INST) 5[illegible]40

1. REFERENCES AND ENCLOSURES	2. TYPE OF PUBLICATION OR PRESENTATION		3. ADMINISTRATIVE INFORMATION
Ref: (a) NRL Instruction 5600.2 (b) NRL Instruction 5510.40E Encl: (1) Two copies of subject publication/presentation	( ) Abstract only, published	( ) Abstract only, not published	STRN NRL/PP/7330-15-2499
	( ) Book author	( ) Book chapter	Route Sheet No. 7330/
	( ) Book editor	( ) Multimedia report	Job Order No. 73-4877-05-5
	(X) Conference Proceedings (refereed)	( ) Conference Proceedings (not refereed)	Classification U ____ S ____ C ____
	( ) Journal article (refereed)	( ) Journal article (not refereed)	FOUO ____
	( ) Oral Presentation, published	( ) Oral Presentation, not published	Sponsor ONR BASE 6.1 6.2
	( ) Video ( ) Poster	( ) Other, explain	Sponsor's approval ____ yes* (attached)
	ALL DOCUMENTS/PRESENTATIONS MUST BE ATTACHED		(*Required if research is other[illegible] 6.1/6.2 NRL or ONR unclassified research or if publication/presentation is classified

4. AUTHOR

Title of Paper or Presentation

Are the satellite-observed narrow, streaky chlorophyll filaments locally intesified by the submesoscale processes?

AUTHOR(s) LEGAL NAMES(s) OF RECORD (First, MI, Last), CODE, (Affiliation if not NRL).

Igor G. Shulman 7331, Bradley Penta 7331, James G Richman 7323, Gregg A. Jacobs 7320, Stephanie C Cayula 7331, Peter Sakalaukus 7331,

This paper will be presented at the SPIE DSS
(Name of Conference)

20-APR - 24-APR-15, Baltimore, MD, Unclassified
(Date, Place and Classification of Conference)

and/or for published in SPIE DSS, Unclassified
(Name and Classification of Publication) (Name of Publisher)

5. CERTIFICATION OR CLASSIFICATION

It is my opinion that the subject paper (is ____) (is not __x__) classified, in accordance with reference (b) and this paper does not violate any disclosure of trade secrets or suggestions of outside individuals or concerns which have been communicated to the NRL in confidence.

This subject paper (has ____) (has never __x__) been incorporated in an official NRL Report.

Igor G. Shulman, 7331
Name and Code (Principal Author) (Legal Name of Record and Signature Only) (Signature)

6. ROUTING/APPROVAL (NOTE: If name other than your legal name of record is annotated on the publication or presentation itself, add an explanatory note in the "comments" section below next to your signed legal name of record)

CODE	SIGNATURE	DATE	COMMENTS
Co-Author(s) Igor Shulman, 7331	I. Shulman	2/25/2015	Need by 18 Mar 2015
			This is a Final Security Review. Any changes made in the document, after approved by Code 1231, nullify the Security Review.
Section Head Richard W. Gould, 7331	R W Gould	2/26/15	
Branch Head Richard L. Croul, 7330	R L Croul	2-26-2015	
Division Head Ruth H. Preller, 7300	Ruth H Preller	2/26/15	1. To the best knowledge of this Division, the subject matter of this publication (has ____) (has never ____) Xbeen classified. 2. This paper (does ____) (does not __X__) contain any militarily critical technology.
ADOR/Director NCST E. R. Franchi, 7000			
DOR/CO			
Security, Code 1231	Sue Fan	3/4/15	A copy of the paper, abstract or presentation is filed in this office.
Associate Counsel,Code 1008.3	[illegible]	3-25-15	
Public Affairs (Unclassified/ Unlimited Only), Code 7030.4	Shannon Mensi	3-12-15	
Division, Code			
Author, Code			

HQ-NRL 5511/6 (Rev. 12/14) THIS FORM CANCELS AND SUPERSEDES ALL PREVIOUS VERSIONS

SAM

ARE THE SATELLITE-OBSERVED NARROW, STREAKY CHLOROPHYLL FILAMENTS LOCALLY INTENSIFIED BY THE SUBMESOSCALE PROCESSES?

Igor Shulman [(1)], Bradley Penta [(1)], James Richman [(1)], Gregg Jacobs [(1)], Stephanie Anderson [(1)], Peter Sakalaukus [(1)]

[(1)] Oceanography Division, Naval Research Laboratory, Stennis Space Center, MS

ABSTRACT

Based on observations and modeling studies we have evaluated the impact of submesoscale processes on the development and intensification of offshore narrow (5-10km wide) phytoplankton filaments during summer time in the Monterey Bay, CA. We have demonstrated that, submesoscale processes (surface frontogenesis and nonlinear Ekman transport) lead to the development of very productive phytoplankton patches along the edges between the cold jet and warm anticyclonic eddy. Our results illustrate that during persistent upwelling favorable winds, submesoscale processes can modulate the development and intensification of offshore narrow (5-10km wide) phytoplankton filaments. These processes can incubate the phytoplankton population offshore (as for example, bioluminescent dinoflagellates during August 2003). These offshore phytoplankton filaments can migrate onshore during relaxed winds following the upwelling, and be an additional source of phytoplankton bloom development in and around Monterey Bay. Therefore, the discussed offshore phytoplankton filaments may be a factor in the Bay ecosystem health, as for example, in the development of such events as harmful algae blooms (HABs). All these emphasize the importance of further observational and modeling studies of these submesoscale processes which impact the development and intensification of offshore phytoplankton filaments.

Keywords: Coastal Processes, Submesoscale Processes, Phytoplankton Filaments, Interdisciplinary Oceanography

Ocean Sensing and Monitoring VII, edited by Weilin W. Hou, Robert A. Arnone, Proc. of SPIE Vol. 9459
94590K · © 2015 SPIE · CCC code: 0277-786X/15/$18 · doi: 10.1117/12.2177569

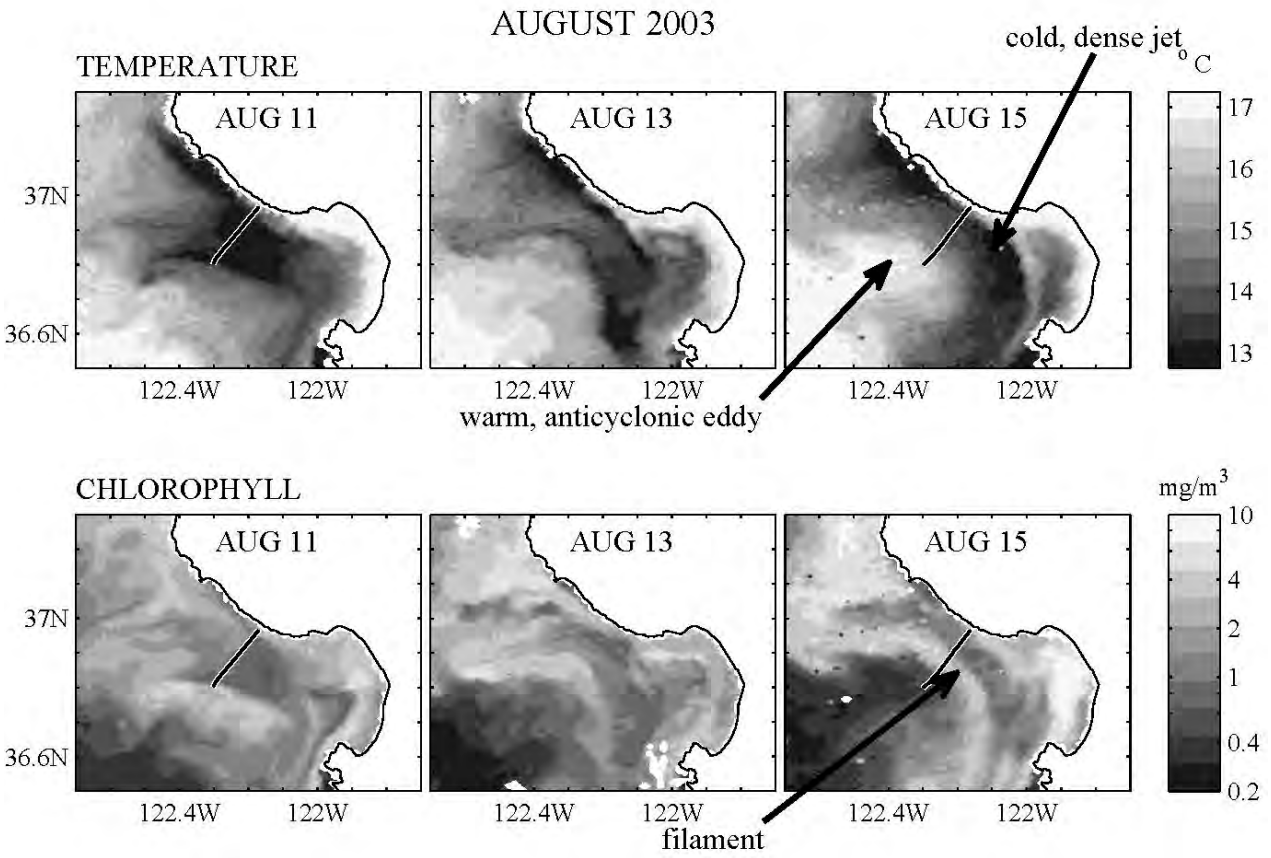

Figure 1. MODIS-Aqua SST and Chlorophyll a images for August 2003. Black lines on MODIS SST and Chlorophyll a images indicate AUV DORADO sections taken 11 and 16 August.

1. INTRODUCTION

Recently there has been an increase in observational and modeling studies focusing on the impact of submesoscale processes on biological dynamics in the ocean (see, for example, review by Levy et al., 2012). It has been found that submesoscale processes with scales of O(1-10km) in the horizontal, O(100m) vertical, and O(1 day) temporal domains impact phytoplankton growth and increase productivity in a variety of ways, as for example, by modulating the vertical supply of nutrients into the euphotic, lighted layer, or by changing the light exposure of phytoplankton by modulating the strength of vertical mixing (see review by Levy et al., 2012). These processes contribute to the development of 5-10 km wide submesoscale filaments in the form of streaky chlorophyll patches often observed in satellite images of ocean

color. As stated in Levy et al (2012), the impact of submesoscale processes on the intensification of phytoplankton filaments depends on the local hydrography, euphotic depth, and nutrient distributions.

During upwelling favorable winds, pockets of cold, salty water appear to the north of Monterey Bay, CA. These pockets grow into a cold, dense jet extending offshore and flowing southward along the entrance to the Bay (Rosenfeld et al., 1994; Ramp et al., 2009). The cold, dense jet interacts with the warmer, less saline anticyclonic circulation offshore. The anti-cyclonic California Current meander, also some-times referred to as the Monterey Bay Eddy (MBE), is a frequently observed feature of the region during the upwelling (Rosenfeld et al., 1994; Ramp et al., 2009). The MODIS-Aqua SSTs for August 11, 13 and 15 of 2003 (Figure 1) illustrate well the described dynamics during the upwelling event: the development and intensification of a southward flowing cold jet and its interaction with the warm offshore anticyclonic circulation. The MODIS-Aqua chlorophyll a images show streaky filaments (5-10km wide) along the offshore edges of the jet (Figure 1). Figure 1 shows that filaments are connected to the high chlorophyll water masses to the north of the Bay, and because of a predominately southward flow during the upwelling, we can suspect that the advection of relatively high chlorophyll water masses from the north contributed to the development of the narrow filaments in Figure 1. At the same time, Figure 1 shows that these narrow filaments are maintained in the frontal area between the meandering warm anticyclonic circulation offshore and the cold jet. It is known (Calil and Richards, 2010; Levy et al., 2012), that the area between a cold jet and warm anticyclonic circulation is prone to generation of submesoscale processes, which contribute to the development of narrow, streaky chlorophyll filaments like those presented in Figure 1. Are the observed streaky chlorophyll a offshore filaments locally intensified by the submesoscale processes?

2. Observations

The MODIS-Aqua satellite imagery was processed using the NRL Automated Processing System (APS) (Gould et al., 2011). In this study, estimates of the chlorophyll *a* (Chl) from MODIS-Aqua imagery for 11-15 August of 2003 were used. Chlorophyll data are derived by OC3M algorithm (O'Reilly et al., 2000) at 1 km pixel resolution. The diffuse attenuation coefficient Kd (488) was estimated in accord with (Lee et al., 2005). The Kd (488) was used to estimate the euphotic depth (noted Eu); the Eu was estimated as the depth where photosynthetic available radiation (PAR) is 1% of its surface value (Lee et al., 2007):

$$Eu = -\ln(0.01)/Kd(488)$$

Observations of winds and PAR from the Monterey Bay Aquarium Research Institute (MBARI) surface moorings M1 (122.02° W, 36.74° N) and M2 (122.40° W, 36.67° N) are used in this study (Figure 2). Near-surface 3m wind speed and direction were measured by a MetSys monitor. The observed PAR was measured by the spectroradiometer mounted on moorings approximately 3m above the water surface (Chavez et al., 2000).

Surface current observations used in this study were derived from the California Coastal Ocean Current Mapping Program's HF radar network (www.cocmp.org). Surface currents were estimated based on inputs from five HF radar sites for August 2003. Vector currents were estimated on a Cartesian grid with a horizontal resolution of 3 km by computing the best-fit vector velocity components using all radial velocity observations within a radius of 3 km for each grid point each hour (Paduan et al., 2006).

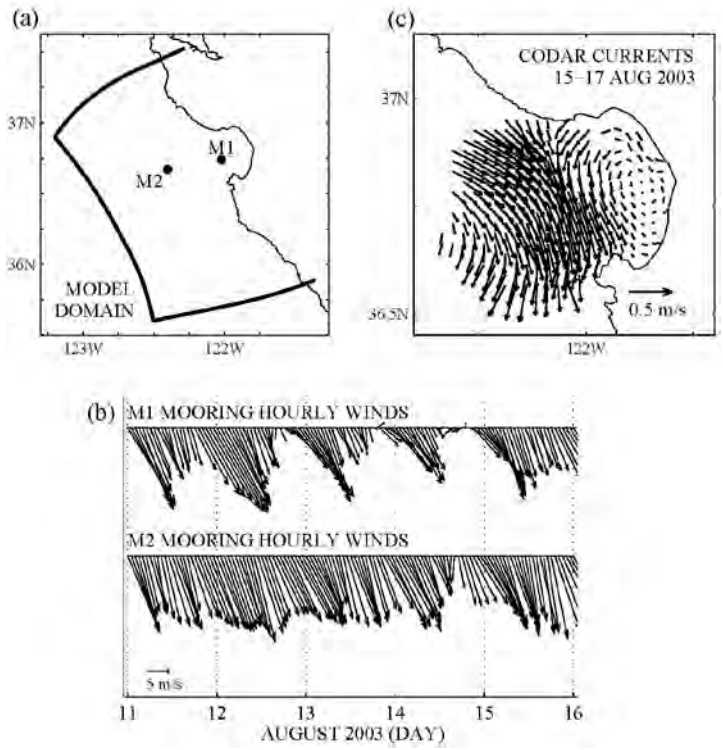

Figure 2. (a) Model domain with locations of moorings M1 and M2. (b) Observed wind velocities at moorings during 11-16 August 2003 and (c) Observed HF Radar surface currents averaged over15-17 August 2003.

Propeller-driven AUV such as the MBARI manufactured DORADO have been described in Bellingham et al, 2000 and Ryan et al, 2009. Deployments of the DORADO during 11 and 16 August 2003 are used in this study. The instruments on board included CTD, optical backscattering, chlorophyll fluorescence, nitrate and bioluminescence potential sensors.

3. Model

The Monterey Bay circulation model used in this study has been described in detail elsewhere (Shulman et al., 2009, 2010). The model domain is shown on Figure 2. The model is based on the Navy Coastal Ocean Model (NCOM), which is a primitive-equation, 3D, hydrostatic model. The Monterey Bay model is forced with surface fluxes from the Coupled Ocean and Atmospheric Mesoscale Prediction System (COAMPS) (Doyle et al., 2009). The Monterey Bay model uses the Navy Coupled Ocean Data Assimilation (NCODA) system. The NCODA assimilates satellite altimeter observations, satellite sea surface temperature, as well as available in-situ vertical temperature and salinity profiles from ships and gliders (Shulman et al., 2009, 2010). In this study, a depth of mixed layer (MLD) is derived from the Monterey Bay model and observations. In both cases, the MLD is computed as the depth at which temperature deviates by 0.3°C from the near surface (at 2m depth) temperature.

4. Results

Because the location of the submesoscale filament (Figure 1) coincides with the area between the cold jet and the anticyclonic circulation offshore, the submesoscale process due to their flow interaction with the development of the surface frontogenesis is considered here (Hoskin, 1982; Levy et al., 2012; Calil and Richards, 2010). Because the upwelling favorable winds have been blowing along the jet and over the anticyclonic circulation for more than a week (Figure 2b), the second submesoscale process considered here is due to the forcing interaction - nonlinear Ekman transport (Thomas and Lee, 2005, Levy et al., 2012; Calil and Richards, 2010). Both submesoscale processes are likely to contribute to the development and intensification of the submesoscale filament (Calil and Richards, 2010; Shulman et al., 2015).

In the first process, the interaction between the dense cold jet and lighter, warmer, anticyclonic circulation leads to an ageostrophic secondary circulation (ASC). These ASC cells are generated in a plane perpendicular to the density front (Hoskins, 1982), which are upward (upwelling) on the light (anticyclonic) side of the front and downward on the dense side of the front. The ASC cells lead to a restratification flow from the light site to the dense. In Hoskin (1982), the vector Q_1 is used to qualitatively diagnose ageostrophic vertical motion due to frontogenesis:

$$Q_1 = (-\frac{\partial u_g}{\partial x}\frac{\partial b}{\partial x} - \frac{\partial v_g}{\partial x}\frac{\partial b}{\partial y}, -\frac{\partial u_g}{\partial y}\frac{\partial b}{\partial x} - \frac{\partial v_g}{\partial y}\frac{\partial b}{\partial y}) \quad (1)$$

Where u_g and v_g are the horizontal geostrophic velocities, and $\frac{\partial b}{\partial x}$ and $\frac{\partial b}{\partial y}$ are the horizontal gradients of buoyancy:

$$b = -g\frac{\rho^*}{\rho_0} \quad (2)$$

with ρ^* being the deviation from the reference density ρ_0, and g is the acceleration due to gravity. The local maximum of Q_1 creates a vertical circulation with associated upwelling/downwelling ACS cells.

The second process is the intensification of ASC cells due to nonlinear Ekman transport (Thomas and Lee, 2005; Levy et al., 2012). This is a result of down-front winds blowing in the direction of the frontal jet. When a wind blows down a front, cross-front advection of density by Ekman flow results in a destabilization of the water column, which results in a convection that is localized to the front. The vertical circulation associated with the ASCs is characterized by subduction on the dense side of the front and upwelling along the frontal interface. It creates upwelling on the anticyclonic circulation site (with negative relative vorticity) and downwelling on the jet site. According to Thomas and Lee (2005), the dominant term in nonlinear Ekman transport is:

$$Me = -\frac{\tau_a}{\rho_0(f+\xi)} \quad (3)$$

Where Me is nonlinear Ekman transport, τ_a is along-front wind stress component, f is Coriolis parameter, and ξ is relative vorticity of geostrophic flow.

The local maxima of Q_1 and Me create a vertical circulation with associated upwelling/downwelling ACS cells. For both processes, ASC cells are upward (upwelling) on the light (anticyclonic) side of the front, and downward on the

dense side of the front. The ASC cells modulate the mixing of material down to the mixed layer depth (MLD), provide injections and cycling of nutrients, as well as the cycling of phytoplankton in the subsurface down to the base of the mixed layer depth. All these directly influence the intensification and development of submesoscale phytoplankton filaments.

Figure 3 shows the model vertical velocity for a section across the cold filament, the warm offshore anticyclonic circulation, and the frontal area between them. The model vertical velocity shows the development of the ACS cell, with the ascending part of this cell coinciding with the warm part of the front. This is in agreement with what would be expected from the surface frontogenesis and nonlinear Ekman transport.

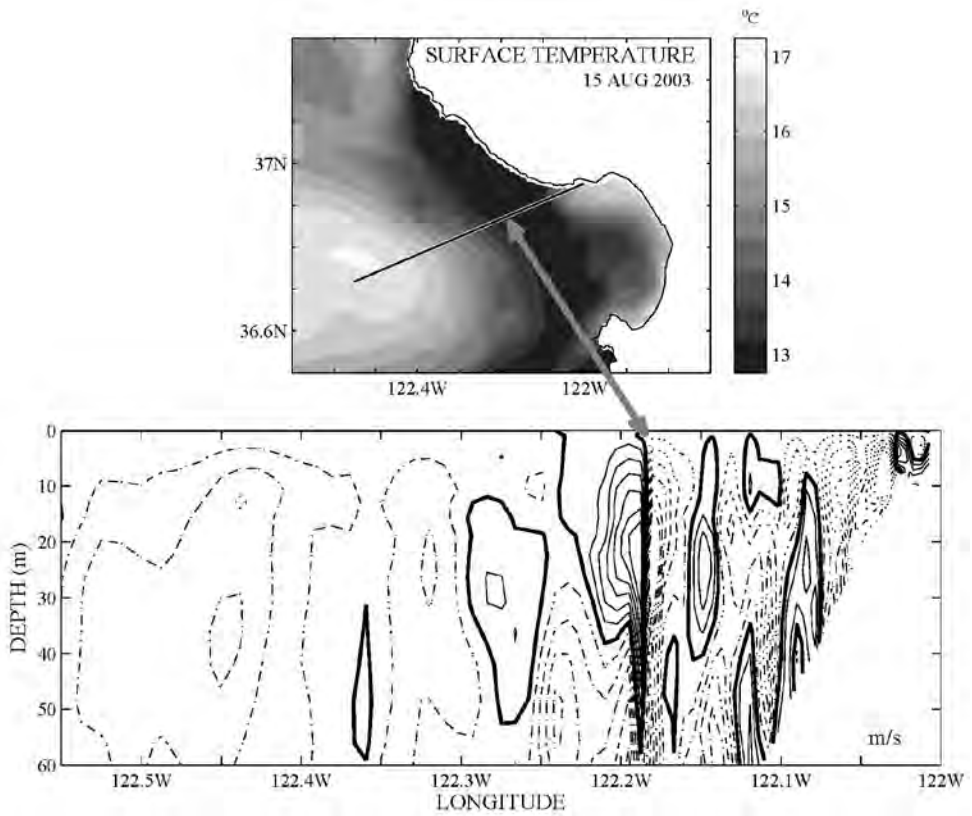

Figure 3. (top panel) the model SST (August 15 2003) with the location of cross section; (bottom panel) the model vertical velocity (solid lines are positive and dashed lines are negative values).

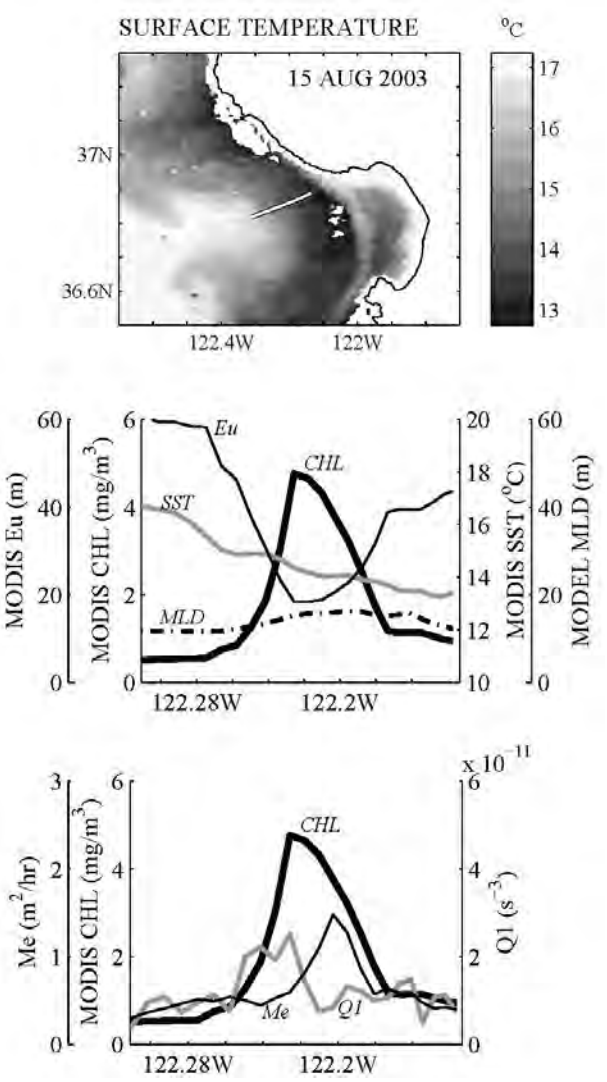

Figure 4. Observed and model predicted properties plotted along sections crossing filament on 15 00Z August 2003. Section is indicated by white line on MODIS-Aqua SST image (top row). Plots along the section of : (second row) MODIS-Agua chlorophyll a, SST, euphotic depth Eu derived from the MODIS-Aqua observations, and the mixed layer depth MLD derived from the model; (third row) MODIS-Agua chlorophyll a, magnitudes of vector Q1, nonlinear Ekman transport Me, which are averaged over top 15m depth.

Figure 4 shows observed and modeled-predicted properties plotted along the section crossing the submesoscale filament. On Figure 4, the vector $Q1$ magnitude (1), the value of nonlinear Ekman transport Me (3) were estimated by using the

COAMPS wind stress and the Monterey Bay model fields of temperature, salinity and velocity averaged over a period of 48 hours centered on August 15 00Z 2003. Estimated values of $Q1$, Me were averaged over the top 15 m depth (Figure 4, third row), which is the depth of model-predicted MLD (Figure 4, second row). Locations of the local maximum of Q1 (1) and Me (3) coincide with the location of the filament.

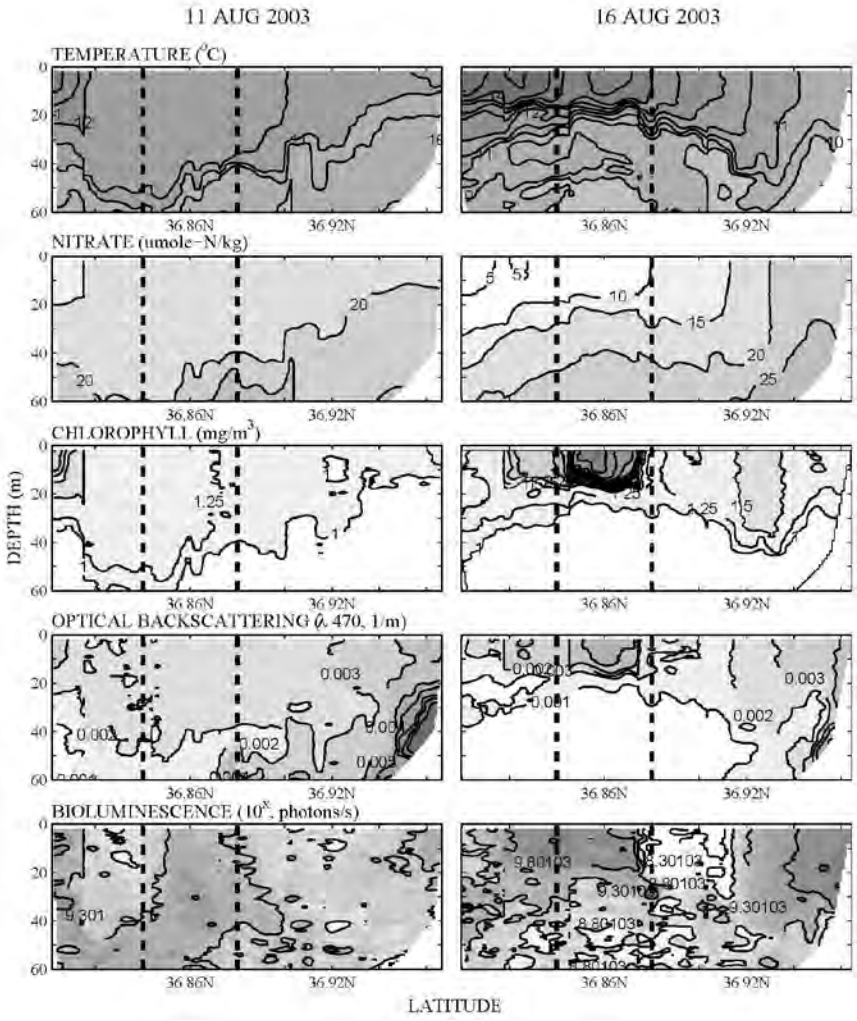

Figure 5. AUV DORADO surveys taken 11and 16 August 2003. Vertical dashed lines indicate location of the high chlorophyll a filament: 11 August- where the filament appeared later on MODIS-Aqua image on 15 August; 16 August – where the filament observed in MODIS-Aqua image on 15 August.

Figure 5 presents subsurface properties along the AUV DORADO surveys. On 16 August, the figure shows the deepening of isotherms offshore at the end of the section where the section reaches the warm, anticyclonic circulation offshore (see position of the section over 15 August MODIS SSTs on Figure 1 of the paper, top panel). Also, there is a flattening of isotherms as the section moves from the warm anticyclonic circulation through the frontal area. This is consistent with the surface frontogenesis, which tends to flatten the isopycnals/isotherms (see, for example, Klein and Lapeyre, 2009). In the area of filament, both model-predicted MLD (~15m, Figure 4, second row) and observed MLD (~15m, Figure 5, 16 August) are shallower then the estimated euphotic depth (Eu) in and around the filament (Figure 4, second row). In this case, the developed ASC cells kept phytoplankton in the lighted area and supported photosynthesis. Also, the ASC cells provided a vertical supply of nutrients into the euphotic area and facilitated consumption of nutrients (see uplifting of nutricline in the area of the filament on 16 August, Figure 5).

In the area of the filament the observed changes in subsurface properties show the shallowing of MLD, increase in consumption of nutrients and increase in subsurface values of chlorophyll, optical backscattering and bioluminescence potential from August 11 to 16 (Figure 6). DORADO surveys (August16) show a coincidence of high values in observed chlorophyll a, BL potential and optical backscattering in the area of the filament. Moline et al, 2009 demonstrated that such a coincidence of high values in considered bio-optical parameters is associated with the presence of bioluminescent species of dinoflagellates in the northern part of the Monterey Bay. Based on this, we suspect that the observed coincidence of high values of chlorophyll a, BL potential and optical backscattering point to a presence of the bioluminescent dinoflagellates in the offshore submesoscale filament.

5. Discussions and Conclusions.

MODIS-Aqua chlorophyll a imagery has demonstrated the development of submesoscale, high chlorophyll a filaments during the upwelling event of August 2003 . These filaments are connected to the high chlorophyll water masses to the north of the Bay (Figure 1), suggesting that the advection of high phytoplankton water masses from the north might have contributed to the development of the observed submesoscale filaments. At the same time, these filaments are confined to the narrow frontal area between the cold jet and the meandering warm anticyclonic circulation offshore. This frontal area is prone to the development of the submesoscale processes and ASC cells, which are known to contribute to the

development of narrow, submesoscale chlorophyll filaments in other areas of the world (see, for example, Calil and Richards, 2010; Levy et al., 2012).

We used the vector Q_1 to diagnose ageostrophic vertical motion due to frontogenesis. The leading order term of nonlinear Ekman transport Me was used to qualitatively diagnose the ageostrophic vertical motion due to nonlinear Ekman transport. Plots of the observed and model-predicted properties across-filament (15 August 2003) have shown locations of the local maximum of Q1 (1) and the nonlinear Ekman transport Me (3) in the area of the observed submesoscale filament (Figure 4). In Shulman et al., 2015, we demonstrated that both submesoscale processes had comparable time scales with the time scales of horizontal advection and with time scales of phytoplankton growth rates documented in the literature.

The observed temperature from the AUV DORADO survey has shown a flattening of isotherms as the section moves from the warm anticyclonic circulation through to the frontal area. This is consistent with the surface frontogenesis, which tends to flatten the isopycnals/isotherms (see, for example, Klein and Lapeyre, 2009).

Because the observed and model-predicted MLD are shallower then the estimated euphotic depth in and around the filament, the developed ASC cells kept phytoplankton in the lighted area and supported photosynthesis. Also, the ASC cells provided a vertical supply of nutrients into the euphotic area and facilitated consumption of nutrients (what was also observed by the DORADO surveys). All of the above indicate that local ASC processes maintained phytoplankton population in the lighted area, supplied nutrient-rich subsurface waters into the euphotic area, and therefore facilitated the intensification and development of the observed phytoplankton rich filament during 11-16 August 2003 (Figure 1).

In Shulman et al., 2015, comparisons of chlorophyll *a* submesoscale filaments on 15 August 2003 and 10 June of 2008 were presented. It was shown that both filaments had similar horizontal across-filament scales. However, the maximum of the June filament chlorophyll *a* was about 3-4 times smaller than in August 2003. The difference between the observed MODIS-Aqua SSTs in August and June does not alone explain the observed 3-4 magnitude difference in the intensity of phytoplankton filaments. Observations have shown that hydrographic conditions and light availability in surface and subsurface were very similar during both of the considered time periods (Shulman et al., 2015). An analysis of water samples collected along the June 2008 filament has shown that conditions were not nutrient (nitrate and silicate) limited for the phytoplankton growth. The mixed layer depth (MLD) along the June filament (~40-60m) was about 2-3 times deeper than the MLD during August 2003 (~15m), and about 10-20m deeper than the estimated euphotic depth.

Therefore, the discussed above submesoscale processes and associated ACS cells mixed the phytoplankton and nutrients below the euphotic depth in June 2008, which provided a slower supply of nutrients into the euphotic depth in comparison to the August 2003 conditions, when the MLD was shallower than the euphotic depth. During June 2008, ACS cells reduced the presence of phytoplankton in the lighted area, and therefore, reduced exposure of phytoplankton to light, and limited the growth of the filament in comparison to August 2003.

Our results show that during the late summer time frame, ASC leads to the development of phytoplankton rich submesoscale filaments offshore, along the edge of the cold jet (when the MLD and euphotic depth are comparable) . Our results illustrate that during persistent upwelling favorable winds, submesoscale processes and ACS cells can modulate the development and intensification of offshore narrow (5-10km wide) phytoplankton filaments. These submesoscale and ACS cells can incubate the phytoplankton population offshore (as for example, bioluminescent dinoflagellates during August 2003). These offshore phytoplankton filaments can migrate onshore during relaxed winds following the upwelling, and provide an additional source of phytoplankton bloom development in and around Monterey Bay. Therefore, the discussed offshore phytoplankton filaments may be a factor in the Bay ecosystem health, as for example, in the development of such events as harmful algae blooms (HABs). All these emphasize the importance of further observational and modeling studies of these submesoscale processes which impact the development and intensification of offshore submesoscale phytoplankton filaments.

Acknowledgments

This research was funded through the Naval Research Laboratory (NRL) under program element 61153N. We thank Drs. Ryan, Chavez and Haddock of MBARI for discussions and providing observations from UUVs and moorings. We thank Brent Bartels of QinetiQ North America for help with the computer code estimating Q1 vector. Computer time for the numerical simulations was provided through a grant from the Department of Defense High Performance Computing Initiative. This manuscript is NRL contribution NRL/PP/7330--15-2499

REFERENCES

Bellingham, J.G., Streitlien, K., Overland, J., Rajan, S., Stein, P., Stannard, J., Kirkwood, W., Yoerger, D., 2000. An Arctic basin observational capability using AUVs, Oceanography 13, 64–71, http://dx.doi.org/10.5670/oceanog.2000.36.

Calil, P. H. R., and K. J. Richards (2010), Transient upwelling hot spots in the oligotrophic North Pacific, J. Geophys. Res., 115, C02003, doi:10.1029/2009JC005360.

Chavez, F.P., Wright, D., Herlien, R., Kelley, M., Shane, F., Strutton, P.G., 2000. A device for protecting moored spectroradiometers from bio-fouling. Journal of Atmospheric and Oceanic Technology 17, 215–219.

Doyle, J. D., Q. Jiang, Y. Chao, and J. Farrara (2009), High-resolution real-time modeling of the marine atmospheric boundary layer in support of the AOSN-II field campaign, Deep Sea Res. Part II, 56, 87–99.

Hoskins, B. J. (1982), The mathematical theory of frontogenesis, Annu. Rev. Fluid Mech., 14, 131–151, doi:10.1146/annurev.fl.14.010182.001023.

Gould, Jr., R.W., S.C. McCarthy, I. Shulman, E. Coelho, and J. Richman. 2011. Estimating Uncertainties in Bio-Optical Products Derived From Satellite Ocean Color Imagery Using an Ensemble Approach. Proc. of SPIE, Remote Sensing of the Ocean, Sea Ice, Coastal Waters, and Large Water Regions 2011, C.R. Bostater, Jr., S.P. Mertikas, Z. Neyt, and M. Velez-Reyes (eds.), Vol. 8175: 817506-01 – 817506-10. doi: 10.1117/12.897614.

Klein, P., and G. Lapeyre (2009), The oceanic vertical pump induced by mesoscale and submesoscale turbulence, Annu. Rev. Mar. Sci., 1,351–375, doi:10.1146/annurev.marine.010908.163704.

Lee, Z. P., K. P. Du, and R. Arnone (2005), A model for the diffuse attenuation coefficient of downwelling irradiance, J. Geophys. Res., 110, C02016, doi:10.1029/2004JC002275.

Lee, Z. P., A. Weidemann, J. Kindle, R. Arnone, K. L. Carder, and C. Davis (2007), Euphotic zone depth: Its derivation and implication to ocean color remote sensing, J. Geophys. Res., 112, C03009, doi:10.1029/2006JC003802.

Levy, M., Ferrari,R., Franks P.J.S, Martin, A. P., Rivière P (2012), Bringing physics to life at the submesoscale, Geophysical Research Letters, VOL. 39, L14602, doi:10.1029/2012GL052756, 2012

Moline, M. A., S. M. Blackwell, J. F. Case, S. H. D. Haddock, C. M. Herren, C. M. Orrico, and E. Terrill, 2009. Bioluminescence to reveal structure and interaction of coastal planktonic communities, Deep Sea Res. II, 56 (3-5), pp. 232-245.

Paduan, J.D., Kim, K.C., Cook, M.S., Chavez, F.P., 2006. Calibration and validation of direction-finding high frequency radar ocean surface current observations. IEEE Journal of Oceanic Engineering, 862–875, DOI: 10.1109/JOE.2006.886195

Ramp S. R., R. E. Davis, N. Leonard, I. Shulman, Y. Chao, A. R. Robinson, J. Marsden, P. Lermusiaux, D. Fratantoni, J.

D. Paduan, F. Chavez, X. S. Liang, W. Leslie, Z. Li, 2009. The Autonomous Ocean Sensing Network (AOSN) Predictive Skill Experiment in the Monterey Bay, *Deep Sea Res. II*, 56 (3-5), pp.8-26.

Rosenfeld, L. K., F. B. Schwing, N. Garfield, and D. E. Tracy (1994), Bifurcated flow from an upwelling center: a cold water source for Monterey Bay. Continental Shelf Research, 14, 931-964.

Ryan, J.P., Fischer, A.M., Kudela, R.M., Gower, J.F.R., King, S.A., Marin III, R., Chavez, F.P., 2009. Influences of upwelling and downwelling winds on red tide bloom dynamics in Monterey Bay, California. Cont. Shelf Res. 29, 785–795, doi:10.1016/j.csr.2008.11.006

Shulman, I., et al. (2009), Impact of glider data assimilation on the Monterey Bay model, Deep Sea Res. Part II, 56, 128–138.

Shulman, I., S. Anderson, C. Rowley, S. deRada, J. Doyle, and S. Ramp (2010), Comparisons of upwelling and relaxation events in the Monterey Bay area, J. Geophys. Res., 115, C06016, doi:10.1029/2009JC005483.

Shulman, I., B. Penta, J. Richman, G. Jacobs, S. Anderson, and P. Sakalaukus (2015), Impact of submesoscale processes on dynamics of phytoplankton filaments, J. Geophys. Res. Oceans, 120, doi:10.1002/2014JC010326.

Thomas, L., and C. Lee (2005), Intensification of ocean fronts by downfront winds, J. Phys. Oceanogr., 35(6), 1086–1102.